K.L. Chapman°, M.N. Glauser° M.S. Reibert▷ & W.S. Saric▷

Proper Orthogonal Decomposition Applied to Boundary-Layer Transition on a Swept Wing

Abstract

Proper orthogonal decomposition (POD), a technique generally used in the study of turbulent flows, is used to analyze experimental signals from multi-point measurements in transitional flow over a 45° swept wing. The data used in this analysis include surface shear stress and two-component velocity measurements from two separate experiments in a highly three-dimensional flow with crossflow-dominated transition. Measurements were obtained across the span at constant chord locations just before and after transition. Streamwise surface shear-stress measurements were acquired through transition to turbulence. The POD solution produces energy-based modes which statistically determine the spatial evolution of the particular flow field. These results reflect physical events in the flow which may provide valuable information to developing flow control strategies.

Experiments

Flow transition is a common phenomenon on aircraft surfaces, particularly on swept wings. The goal of this research effort is to use proper orthogonal decomposition (POD) to statistically capture swept-wing flow evolution in space from multi-point measurements. The data used in this analysis were obtained via multi-element hot-film and cross-wire anemometry on a 45° swept wing (shown in Fig. 1) with a chord length of $c = 1.83$ m at the Arizona State University Unsteady Wind Tunnel facility. Wall liners, contoured to the inviscid streamlines,

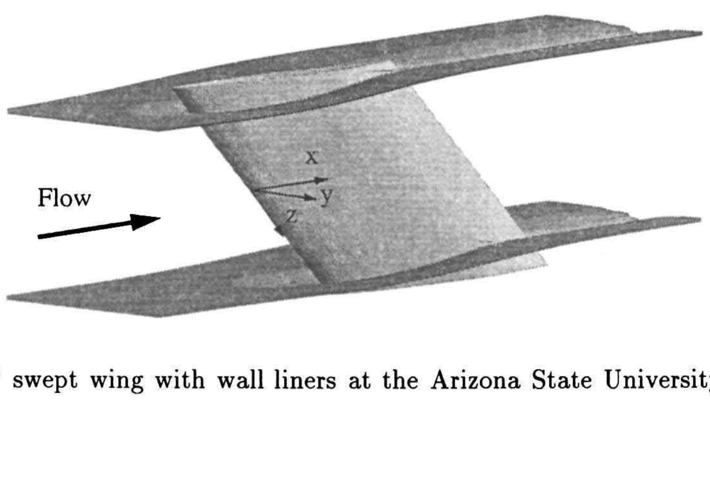

Figure 1: 45° swept wing with wall liners at the Arizona State University Unsteady Wind Tunnel.

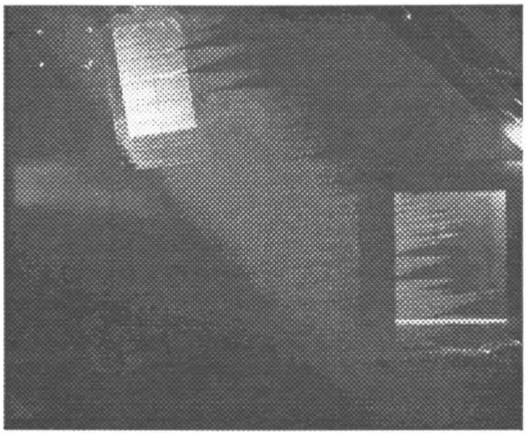

Figure 2: Dagenhart *et al.* (1989) experiment: Placement of hot-film array with naphthalene surface flow visualization results shown. Flow is left to right.

are used to simulate a wing of infinite span. The experiments were designed to produce a highly three-dimensional flow consisting of stationary crossflow vortices which dominate transition starting near $x/c = 0.52$ at a Reynolds number of $Re_c = 2.4 \times 10^6$. Naphthalene surface flow visualization and single hot-wire velocity scans are used to determine the boundary-layer state.

An experiment performed by Dagenhart *et al.* (1989) included spanwise surface shear-stress measurements in the laminar regime and streamwise measurements through transition. The surface-mounted hot-film arrays were aligned to the visualized crossflow vortex axis as shown in Fig. 2. The crossflow array consisted of 13 sensors spaced 1.3 mm apart, covering a range of 15.3 mm in span. The streamwise array consisted of 13 hot-film sensors spaced 2.54 mm apart, covering a range of 30.48 mm. For a more detailed description of this experiment, refer to Dagenhart *et al.* (1989).

A second experiment by Chapman *et al.* (1996) was based on the analysis of the Dagenhart experiment and designed with the POD technique in mind. A series of 6 μm thick roughness elements spaced 12 mm apart were placed downstream of the attachment line across the entire span at $x/c = 0.023$ to force the dominant crossflow vortex wavelength, thus isolating the dominant mode in the flow. The data acquired from this experiment included two-point, two-component velocity measurements in span at two chord locations; at $x/c = 0.50$, just before transition, and at $x/c = 0.58$ in the turbulent region. These correlation measurements (outlined in Fig. 3) for each of the two chord locations were made at a single height of $y = 3.0$ mm in the boundary layer at 8 span locations spaced 4 mm apart. The cross-wire measurements were taken above surface-mounted hot-film arrays used to supplement the data from the Dagenhart experiment. Only the cross-wire data will be analyzed here. Refer to Chapman *et al.* (1996) for a more detailed description of the experiment.

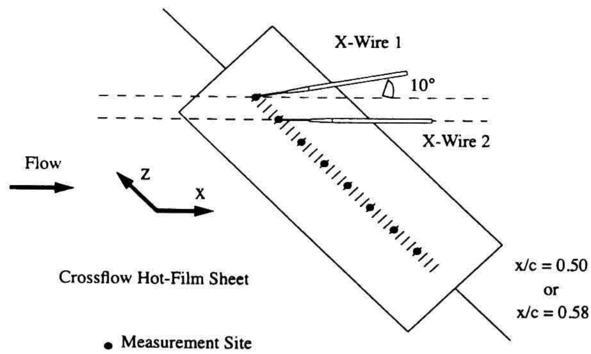

Figure 3: Chapman *et al.* (1996) experiment: Schematic of cross-wire experiment at x/c=0.50 and x/c=0.58 with crossflow hot-film sheets used to define measurement grid points.

Proper orthogonal decomposition

Proper orthogonal decomposition (POD) is a mathematically unbiased method for extracting a system of eigenfunctions through the solution of an integral eigenvalue equation. It was introduced to the study of inhomogeneous turbulent flows by Lumley (1967) as a way of identifying large-scale structures, i.e., those events in the flow which have the largest mean-square projection on the flow field. In general, it is an objective method that decomposes a system of signals into various modes on an energy basis without imposing a basis set as in Fourier decomposition, but determines the appropriate modes directly from the data. Hence, POD includes the results of the flow non-linearities in the solved eigenfunctions, unlike conventional linear-theory methods. For a summary of POD and applications in turbulence, refer to Berkooz *et al.* (1993).

Lumley (1967) defined coherent structures as those events in the flow with the largest mean-square projection on the random velocity field, i.e., those with the maximum energy. Defining $\vec{\phi}(\vec{x},t)$ as the candidate structure and maximizing this projection leads to the following integral eigenvalue problem:

$$\int\int\int\int R_{ij}(\vec{x},\vec{x}',t,t')\phi_j^{(n)}(\vec{x}',t')d\vec{x}'dt' = \lambda^{(n)}\phi_i^{(n)}(\vec{x},t), \qquad (1)$$

with a symmetric kernel that is the velocity cross-correlation tensor,

$$R_{ij}(\vec{x},\vec{x}',t,t') = \overline{u_i(\vec{x},t)u_j(\vec{x}',t')}. \qquad (2)$$

The eigenvalues, $\lambda^{(n)}$, which represent an energy distribution across the POD modes, $\phi^{(n)}(\vec{x},t)$, reflect the projection. Theoretically, Eq. (1) has an infinite number of orthonormal solutions. However, it is maximally discretized experimentally to the number of measurement sites.

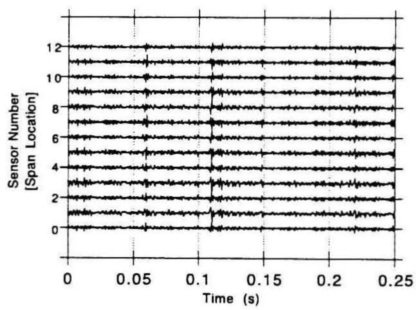

Figure 4: Simultaneously measured spanwise hot-film time histories in the laminar regime. Sensor spacing is 1.3 mm.

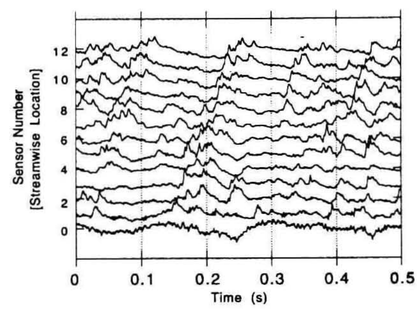

Figure 5: Simultaneously measured streamwise hot-film time histories through transition. Sensor spacing is 2.54 mm.

In this study, POD is applied to the surface shear-stress measurements of the Dagenhart experiment and to the two-component velocity measurements of the Chapman experiment, treating each component independently. Therefore, for these scalar solutions, Eq. (1) becomes

$$\int R_{11}(x,x')\phi_1^{(n)}(x')dx' = \lambda^{(n)}\phi_1^{(n)}(x), \quad (3)$$

where the discrete variable, n, is the POD mode number maximally discretized to the number of measurement sites. Note that in Eq. (3), R_{11} is formed with either shear stresses or velocities and x denotes the coordinate in either the spanwise or streamwise measurement grids, as appropriate, since each data set is treated as an independent system. Only the one-dimensional POD solution is presented here. From these solutions, it is possible to statistically determine the spatial evolution of the eigenmodes across each measurement range.

Proper orthogonal decomposition results

Surface shear-stress solutions

POD was applied to the spanwise surface shear-stress data in the laminar regime shown in Fig. 4 and to the streamwise surface shear-stress data through transition shown in Fig. 5. The solutions are obtained using two-point correlation tensors normalized by the appropriate root-mean-square values.

In Fig. 6, the resulting eigenvalues plotted as a function of POD mode number for these data show the contribution of each mode to the total energy of the measured surface shear-stress fields. The spanwise eigenvalues contain 98% of the total energy in the first three modes, whereas only 69% of the total energy

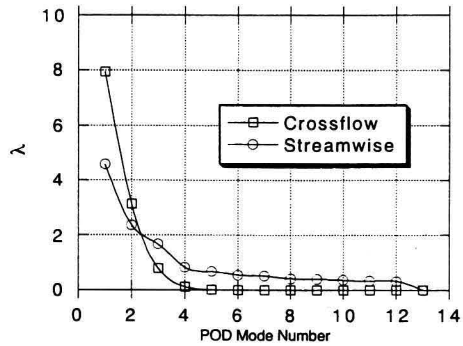

Figure 6: Eigenvalues from the one-dimensional POD solution for the surface shear-stress data showing the energy distribution across POD modes for each regime.

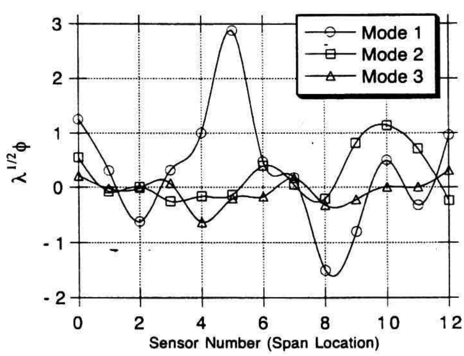

Figure 7: Spatial evolution of the first three spanwise modes in the laminar regime.

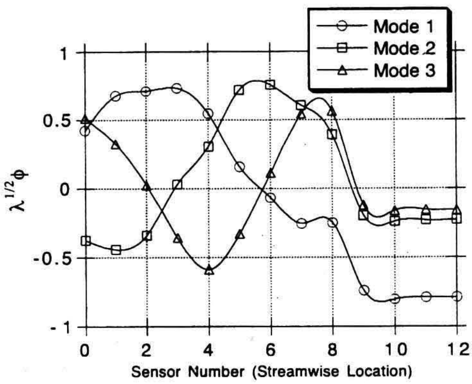

Figure 8: Spatial evolution of the first three streamwise modes through transition.

is in the first three modes of the streamwise solution. In fact, six modes are needed to represent over 80% of the field's total measured energy. Thus, the use of higher modes in the analysis of transitional flows is a necessity.

The first three eigenfunctions for the spanwise and streamwise solutions are plotted in Figs. 7 and 8, respectively, and are weighted by $\lambda^{1/2}$ to distinguish them as characteristic surface shear stresses. High modal amplitudes statistically correspond to regions of high shear. The spatial evolution of the first spanwise mode in Fig. 7 captures the dominant wavelength of the co-rotating crossflow vortices, determined to be approximately 9.0 mm from flow visualizations and mean-velocity boundary-layer scans. Hence, the spatial wavelength is expected to span across seven hot-film sensors. This is captured by the first mode from sensor number 2 through 8 inclusive. A second vortex of weaker amplitude is also captured by the first two modes from sensors 8 through 12 inclusive. In the cross-wire experiment, this type of non-uniformity of the vortices was removed through the use of roughness elements, effectively isolating the wavelength to

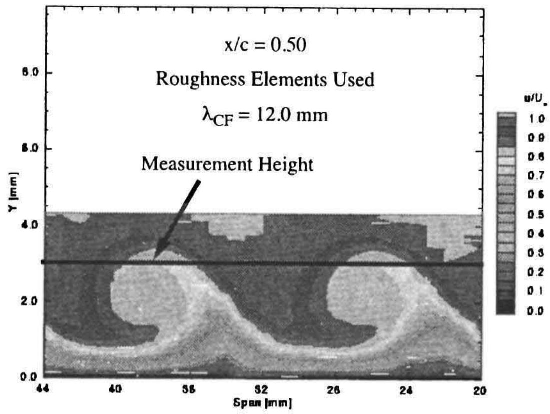

Figure 9: Typical mean velocity contour plot of stationary crossflow vortices (2:1 scale).

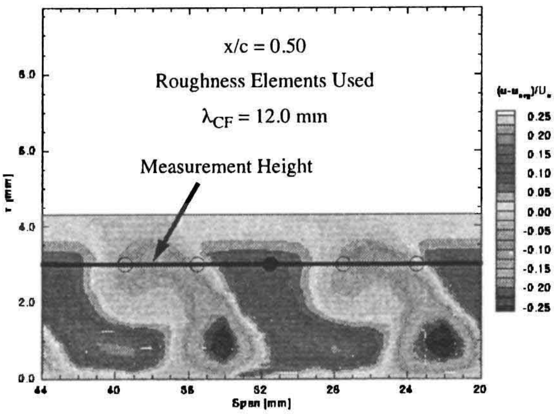

Figure 10: Typical disturbance contour plot of stationary crossflow vortices (2:1 scale).

the first mode. Higher spanwise modes provided very little information.

The spatial evolution of the streamwise modes in Fig. 8 reveal important characteristics of flow transition. From observation of the time history data in Fig. 5, one sees the onset of turbulence occurring near sensor number 9. This event is dramatically captured in the first three eigenmodes. The functions spatially evolve from high amplitude periodic waveforms to fairly constant values at the onset of turbulence. The fact that the first three modes are at the same amplitude in the transition region supports the absolute need for the inclusion of higher modes when modelling this regime. It also suggests that the dominant three modes are of equal importance. In the turbulent regime, the energy in the flow becomes organized and may be adequately represented by simply the first three modes. This is comparable to other POD applications in turbulent flows where increasing mode number reflects a significant decrease in energy. Therefore, the solution of the POD through transition to turbulence statistically reveals a spatial organization of energy which requires higher modal information in transitioning regions, but needs only the first three modes in turbulent regimes.

Individual velocity component solutions

The POD was also applied to the two-point cross-wire data taken at a height of $y = 3.0$ mm in the boundary layer. Fig. 9 shows a typical mean velocity contour plot of the stationary crossflow vortices obtained by single hot-wire scans. Fig. 10 is a statistical picture of the flow disturbances, i.e., the fluctuations about the mean, for the data shown in Fig. 9. The physics of the solved eigenfunctions at $y = 3.0$ mm can then be appropriately mapped to this plot.

The eigenvalues for the u and w components of velocity are shown in Fig. 11 for $x/c = 0.50$ and $x/c = 0.58$. The turbulent solutions are at an entirely higher energy level suggesting the fluctuating components have acquired more energy

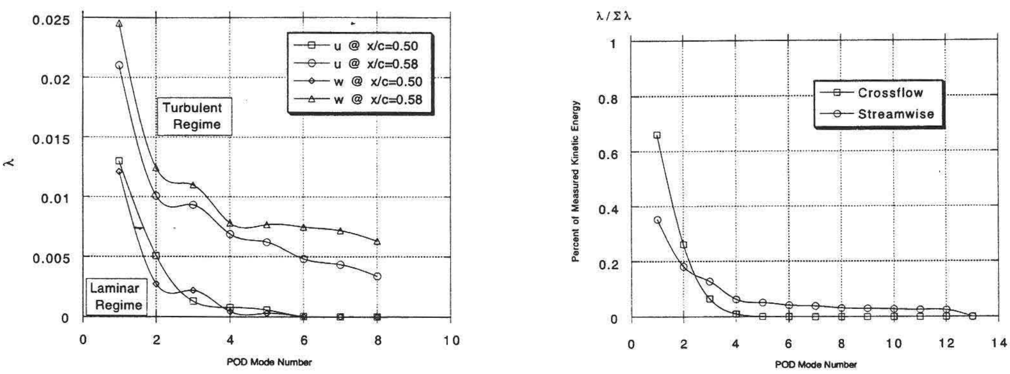

Figure 11: Eigenvalues from the one-dimensional POD solution for the velocity component data.

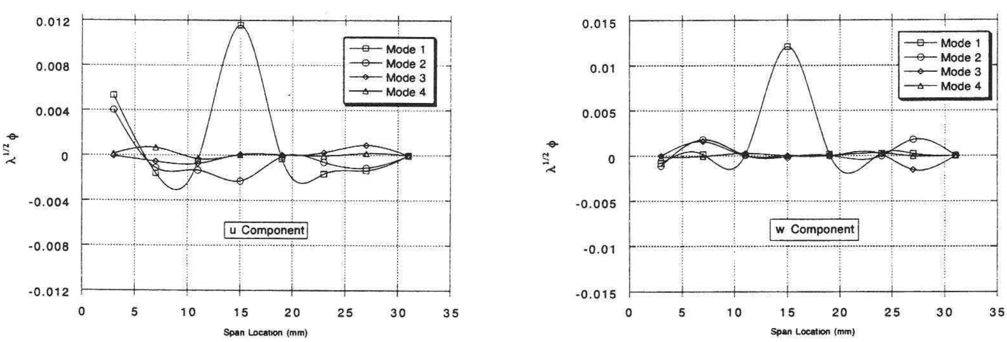

Figure 12: Spatial evolution of the first four eigenmodes for both u and w velocity components in the laminar regime at $x/c = 0.50$.

from the mean flow. Also, the eigenvalues demonstrate that only the first three POD modes are significant in the laminar regime, yet higher modes are active in the turbulent regime, consistent with the shear-stress analysis.

The spanwise evolution of the first four eigenmodes of both components in the laminar regime, shown in Fig. 12, demonstrate the effectiveness of the POD in capturing the crossflow vortex wavelength of $\lambda_{CF} = 12$ mm entirely in the first mode. The vortex structure in the first mode ranges from 7 mm to 19 mm on the measurement grid which can be mapped to the disturbance contour plot in Fig. 10. The circles in Fig. 10 represent five typical measurement points that could be characterized by the five eigenfunction points ranging from 7 mm to 27 mm for the first modes of each component in Fig. 12. In this range, the first modes show two points of relatively low disturbances (each represented by o in Fig. 10) followed by a large amplitude event (represented by • in Fig. 10) and then two more points of relatively low amplitude velocity disturbances.

The spanwise evolution of the first four eigenmodes for the u and w compo-

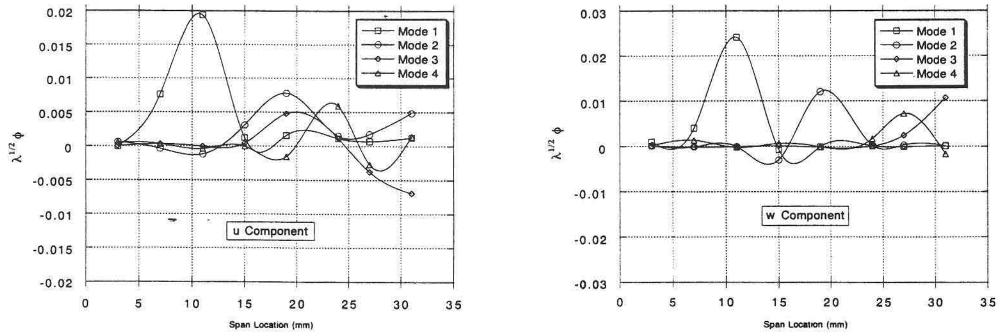

Figure 13: Spatial evolution of the first four eigenmodes for both u and w velocity components in the turbulent regime at $x/c = 0.58$.

nents in the turbulent regime are shown in Fig. 13. The same events in the first modes of the laminar solution which capture the crossflow vortex wavelength are retained and increase in amplitude in the turbulent solutions. This suggests that the initial structures present in the flow field before transition acquire energy and remain intact in the turbulent regime. Flow visualization results show the crossflow vortex axis to be angled approximately 6° from the x coordinate axis thus explaining the 4 mm shift of the vortex structure position (from 15 mm at $x/c = 0.50$ to 11 mm at $x/c = 0.58$). The turbulent solution shows higher modes are now significant and have amplitudes nearly half of the first mode.

Conclusions

Proper orthogonal decomposition has been shown to be a useful and objective tool in analyzing transitional flow. Large scale events, such as the crossflow vortex wavelength are easily tracked and can be used for structure identification purposes where supplemental experiments such as flow visualization are not available. The POD modes clearly identify the onset of turbulence when applied to multi-point streamwise measurements. The POD solution provides a set of eigenfunctions decomposed on an energy basis which can then be used in developing flow control strategies and flow models.

Acknowledgements

This work is supported under NASA Grant NAG2-724 by NASA Dryden Flight Research Center. The authors would like to thank Mssrs Dan Clevenger, Edmund Hamlin, and Paul Harney for their contributions to this research effort.

References

Berkooz, G., Holmes, P. & Lumley, J. L. 1993 – The proper orthogonal decomposition in the analysis of turbulent flows. *Ann. Rev. Fluid Mech.* **25**, 539-575.

Chapman, K.L., Glauser, M.N., Reibert, M.S. & Saric, W.S. 1996 – A multipoint correlation analysis of a crossflow-dominated boundary layer. AIAA 96-0186.

Dagenhart, J.R., Saric, W.S., Mousseux, M.C. & Stack, J.P. 1989 – Crossflow-vortex instability and transition on a 45-degree swept wing. AIAA 89-1892.

Lumley, J.L. 1967 – The structure of inhomogeneous turbulent flows. *Atmos. Turb. and Radio Wave Prop.*, edited by Yaglom & Tatarsky, Nauka, Moscow, pp. 166-176.

Rempfer, D. 1996 – Investigations of boundary layer transition via Galerkin projections on empirical eigenfunctions. *Phys. Fluids* **8**, 175-188.

Saric, W.S. 1994 – Low-speed boundary-layer transition experiments. *Transition: experiments, theory and computations*, edited by Corke, Erlebacher & Hussaini, Oxford Press.

Authors' addresses

°Clarkson University
Mechanical and Aeronautical Engineering
Box 5725
Potsdam, NY 13699, USA

▹Arizona State University
Mechanical and Aerospace Engineering
Box 87-6106
Tempe, AZ 85287-6106, USA